Integrated finite element models for aeroelastic analysis and piezoelectric energy harvesting in bladeless wind turbines

Mohamed Mahran Kasem[1,2*], Ahmed Elbaz[3]

[1]School of Engineering and Applied Science, Nile University, Shaikh Zayed City 12588, Egypt.
[2]Aerospace Engineering Department, Cairo University, Giza 12613, Egypt.
[3]Faculty of Engineering, The British University in Egypt, Cairo, 11837, Egypt.

Corresponding author: Mohamed Mahran Kasem (*Email: mkasem@nu.edu.eg*)

Abstract

Two novel finite element models (FEMs) have been developed to analyze bladeless wind turbines (BWTs): one focusing on aeroelastic analysis and the other on piezoelectric energy harvesting. The aeroelastic model simulates the interaction between aerodynamic loads and the BWT structure, utilizing a semi-empirical wake oscillator model to generate aerodynamic loads while solving the structural equations using FEM. The piezoelectric energy harvesting model predicts the effects of applying sinusoidal aerodynamic loads on the charge generated by piezoelectric patches placed at the root of a plate-like BWT. The aeroelastic model effectively predicts the aeroelastic characteristics of BWTs, providing insights into their stability and performance under various wind conditions. Meanwhile, the piezoelectric energy harvesting model efficiently simulates the energy conversion phenomena, demonstrating the potential for harnessing electrical energy from the mechanical vibrations of BWTs using smart piezoelectric patches that are mounted at the root of a plate-like BWT. These models offer valuable tools for optimizing the design and functionality of BWTs in renewable energy applications.

Keywords: Aeroelasticity, Bladeless wind turbine, Finite element method, Piezoelectric energy harvesting.

Competing Interests: The authors declare that they have no competing interests.
Authors' Contributions: Both authors contributed equally to the conception and design of the study. Both authors have read and agreed to the published version of the manuscript.
Transparency: The authors confirm that the manuscript is an honest, accurate, and transparent account of the study; that no vital features of the study have been omitted; and that any discrepancies from the study as planned have been explained. This study followed all ethical practices during writing.

1. Introduction

Bladeless wind turbines (BWTs) offer a groundbreaking alternative for harnessing wind energy by utilizing the principles of vortex-induced vibrations (VIV) instead of the traditional rotating blades found in conventional turbines. A typical BWT consists of a foundation beam supporting a mast, which provides an aerodynamic shape and serves as the

primary component exposed to wind. The mast integrates tuning mechanisms and electromagnetic devices to adjust its natural frequency and convert vibrations into electrical energy. Typically constructed from lightweight, stiff materials such as composites, the mast can have cylindrical or tapered shapes. Tapered designs are particularly advantageous, as they exhibit broader lock-in ranges and hybrid vortex shedding behaviors. The foundation beam, often made from iron, steel, or carbon fiber, anchors the mast while accommodating its cantilevered motion. Meanwhile, the tuning and electrical systems—comprising springs, dampers, and electromagnetic devices—ensure efficient operation and energy generation across varying wind conditions. Unlike traditional turbines, BWTs eliminate rotating blades, resulting in quieter, safer operation and reduced maintenance requirements [1, 2].

BWTs operate on the principle of VIV, which occurs when airflow around a bluff body creates alternating low-pressure vortices, causing the body to oscillate perpendicular to the wind direction. Factors such as body geometry, Reynolds number, Strouhal number, and vortex shedding frequency significantly influence energy conversion efficiency [3]. Additionally, three interrelated aerodynamic phenomena impact BWT performance [4] including (1) Vortex-Induced Vibrations (VIV): Oscillations caused by alternating vortex shedding, dependent on parameters like Strouhal number, Reynolds number, and the structure's natural frequency, (2) Galloping: A self-excited vibration seen in non-circular bluff bodies, driven by aerodynamic instability and characterized by large, low-frequency oscillations, and (3) Flutter: Oscillations arising from interactions between aerodynamic forces and structural elasticity, potentially leading to structural failure. While distinct, these phenomena share a common reliance on resonance between the turbine and surrounding airflow frequencies. Analyzing BWTs requires advanced modeling to capture air-structure interactions.

Several studies have advanced the understanding of BWT dynamics. Berger [5] Explored vortex-excited oscillations in circular cylinders, analyzing phase relationships between lift forces and cylinder displacement. The study emphasized nonlinear feedback mechanisms and their impact on stability and oscillation amplitude. Skop and Griffin [6] Developed an empirical model using a modified Van der Pol equation to predict resonant transverse oscillations in bluff bodies, with parameters calibrated through experimental data. Later enhancements by Skop and Balasubramanian [7] refined the model, incorporating nonlinear terms to improve accuracy. Chizfahm, et al. [8] Presented dynamic models for BWT configurations using Euler-Bernoulli beam theory and the Galerkin method. Their findings revealed that conic BWTs perform better at high wind speeds, while cylindrical designs excel at lower speeds, highlighting the significance of structural design in optimizing energy harvesting efficiency. This comprehensive body of research underscores the potential of BWTs as a transformative technology in wind energy generation, offering improved safety, reduced environmental impact, and enhanced adaptability to varying wind conditions.

The integration of smart elements such as piezoelectric materials is found to improve the overall efficiency of energy harvesting. By combining piezoelectric and electromagnetic effects, hybrid models can take advantage of the high efficiency of piezoelectric materials at small deformations and the high-power density of electromagnetic systems at larger deformations. The phenomenon of piezoelectricity, discovered by Pierre and Jacques Curie in 1880, involves the generation of an electric field in response to mechanical stress in certain crystals. This effect is utilized in energy harvesting devices to convert mechanical energy into electrical energy. Piezoelectric materials like PZT (lead-zirconate-titanate) and PVDF (polyvinylidene fluoride) are commonly used due to their high sensitivity and flexibility. The fundamental equations of piezoelectricity involve stress, electric field, and the respective material properties, governed by the piezoelectric tensor [9]. The application of piezoelectric energy harvesting in BWT is not common in research and it can help increase the energy extracted from BWTs.

Piezoelectric energy harvesting (PEH) has emerged as a promising technology for converting mechanical vibrations into electrical energy, leveraging the unique properties of piezoelectric materials to meet low-power demands. The concept has been extensively explored in aeroelastic systems, where fluid-structure interactions like flutter and vortex-induced vibrations (VIV) are exploited. Studies have shown that flutter-induced limit-cycle oscillations (LCO) significantly enhance energy output, as demonstrated in nonlinear analyses that optimize spring coefficients to maximize power while avoiding subcritical instabilities [10-12]. Similarly, Akaydin, et al. [13] illustrated the potential of VIV-based harvesters by synchronizing the natural frequency of piezoelectric structures with vortex shedding frequencies in turbulent flows [13]. Modeling approaches, such as finite element methods (FEM) and lumped-parameter models, have proven crucial in capturing the dynamics of these systems, enabling geometric and material optimization [14]. Stability characterization methods further ensure reliable operation under varying aerodynamic conditions [15, 16]. Experimental validation has demonstrated that PEH systems, such as cantilevered beams and triangular-section galloping harvesters, can achieve high efficiency, particularly when load resistance and system parameters are tuned for optimal performance [17].

Despite the extensive research on BWTs, limited studies have focused on developing FE models for their analysis and design. This work aims to bridge that gap by offering a comprehensive understanding of the principles underlying BWTs, their components, dynamic behavior, and piezoelectric energy harvesting mechanisms using the FEM. Two distinct models are developed and analyzed: one employing a beam element FE approximation and the other utilizing a plate element FE approximation.

2. Aerodynamic Modes

To ensure maximum vibration in BWTs, four key factors must be addressed. Firstly, the structural natural mode of the turbine must match the vortex shedding frequency, ensuring that the turbine resonates with the aerodynamic forces. Secondly, the aerodynamic characteristics of the turbine, including the lift and drag forces, must be carefully considered to optimize the interaction with the airflow. Thirdly, the structural properties, such as stiffness and damping, need to be precisely tuned to sustain and amplify the induced vibrations. Finally, the interaction between the aerodynamic forces and

the structural response must be thoroughly analyzed and modeled to predict and control the resonance phenomena. By addressing these four critical issues, we can maximize the vibrations of the BWTs, thereby enhancing its energy capture and overall efficiency.

For resonance to occur in a BWT, one of the structural fundamental frequencies must equal the vortex shedding frequency. The structural natural modes can be determined by approximating the BWT as a cantilever beam, using either analytical methods or finite element (FE) solutions. On the other hand, the aerodynamic vortex shedding frequency can be derived through empirical formulas or Computational Fluid Dynamics (CFD). By aligning the structural natural frequency with the vortex shedding frequency, the turbine can achieve resonance, leading to amplified vibrations and optimized energy harvesting. This approach ensures that the BWT operates efficiently by fully leveraging the aerodynamic forces acting on it.

The aerodynamic modes, or the vortex shedding frequency, can be obtained through empirical relations or CFD simulations. For the empirical relation, the vortex shedding frequency can be determined using the following equation:

$$\omega_s = 2\pi S_t \frac{U}{D} \tag{1}$$

S_t is the Strouhal number that can be defined based on empirical value ($S_t = 0.15 - 0.21$).

Another method for obtaining the aerodynamic frequency is by employing the CFD simulation. In CFD analysis, we are solving Navier-Stokes equations. The Navier-Stokes equations for modeling laminar, unsteady 2D flow over a cylinder are a set of partial differential equations that describe the motion of the fluid. These equations include the continuity equation and the momentum equations in x and y directions.

2.1. Continuity Equation

$$\frac{\partial U}{\partial x} + \frac{\partial V}{\partial y} = 0 \tag{2}$$

Where U and V are velocity components in x and y directions, respectively.

2.2. Momentum Equations
In x-direction

$$\frac{\partial U}{\partial t} + U\frac{\partial U}{\partial x} + V\frac{\partial U}{\partial y} = -\frac{1}{\rho}\frac{\partial P}{\partial x} + \nu\left(\frac{\partial^2 U}{\partial x^2} + \frac{\partial^2 U}{\partial y^2}\right) \tag{3}$$

2.3. In Y-Direction

$$\frac{\partial V}{\partial t} + U\frac{\partial V}{\partial x} + V\frac{\partial V}{\partial y} = -\frac{1}{\rho}\frac{\partial P}{\partial x} + \nu\left(\frac{\partial^2 V}{\partial x^2} + \frac{\partial^2 V}{\partial y^2}\right) \tag{4}$$

Where P is the pressure, ρ is the flow density and ν is the flow viscosity.

Those are three nonlinear PDEs that are solved by iteration using finite volume method by implementing a proper CFD code, and by applying the boundary conditions, Figure 1 shows the computational domain used to study the flow around the BWT model. The domain is 50 m in diameter. The flow is assumed to be two dimensional.
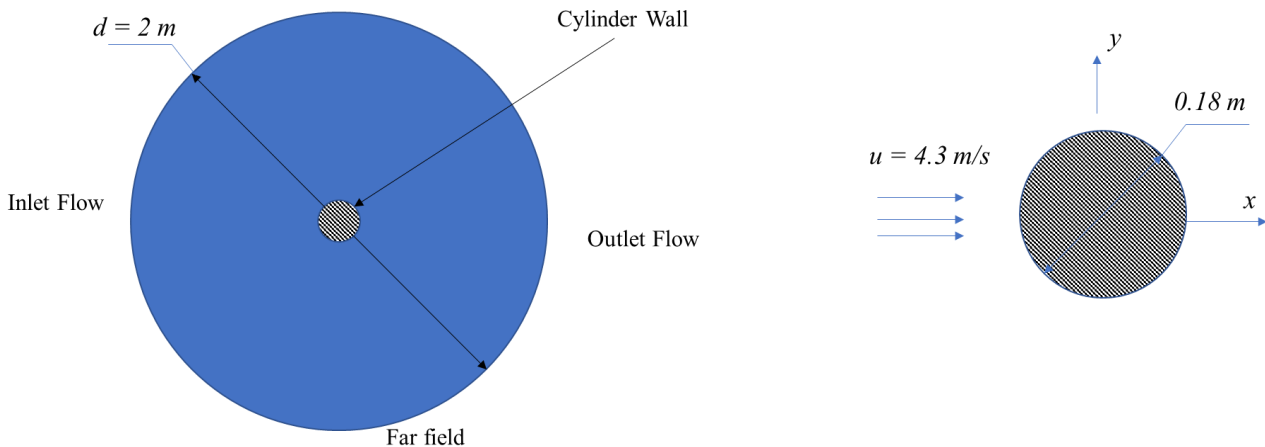

Figure 1.
CFD computational domain.

For predicting the vortex-shedding frequency using CFD simulation a proper time-step and computational time should be selected to determine the vortex-shedding phenomena. Figure 2 shows the excitation of lift coefficient for a typical 2D cylinder with 0.18 m diameter, and velocity 4.3 m/s. The maximum fluid induced lift coefficient is about $C_{L0} = 0.165$ whereas the vortex shedding frequency is determined to be $42.2 \frac{rad}{s}$. This information will be used in the following sections for the aeroelastic analysis using the FEM.
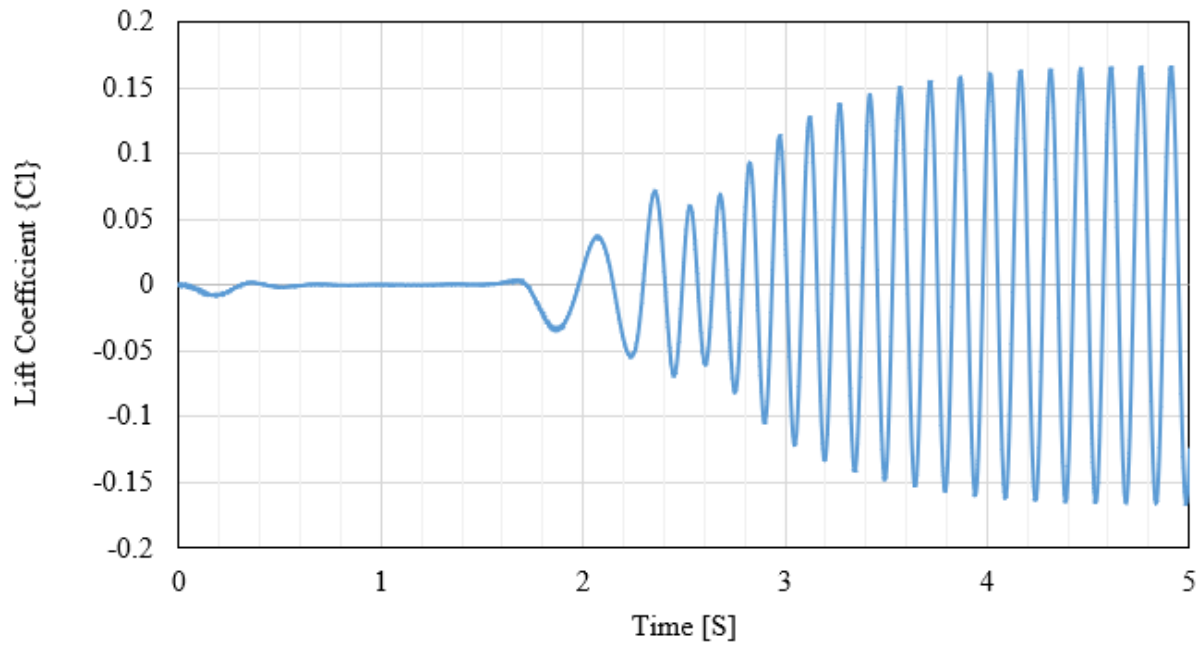

Figure 2.
Lift coefficient.
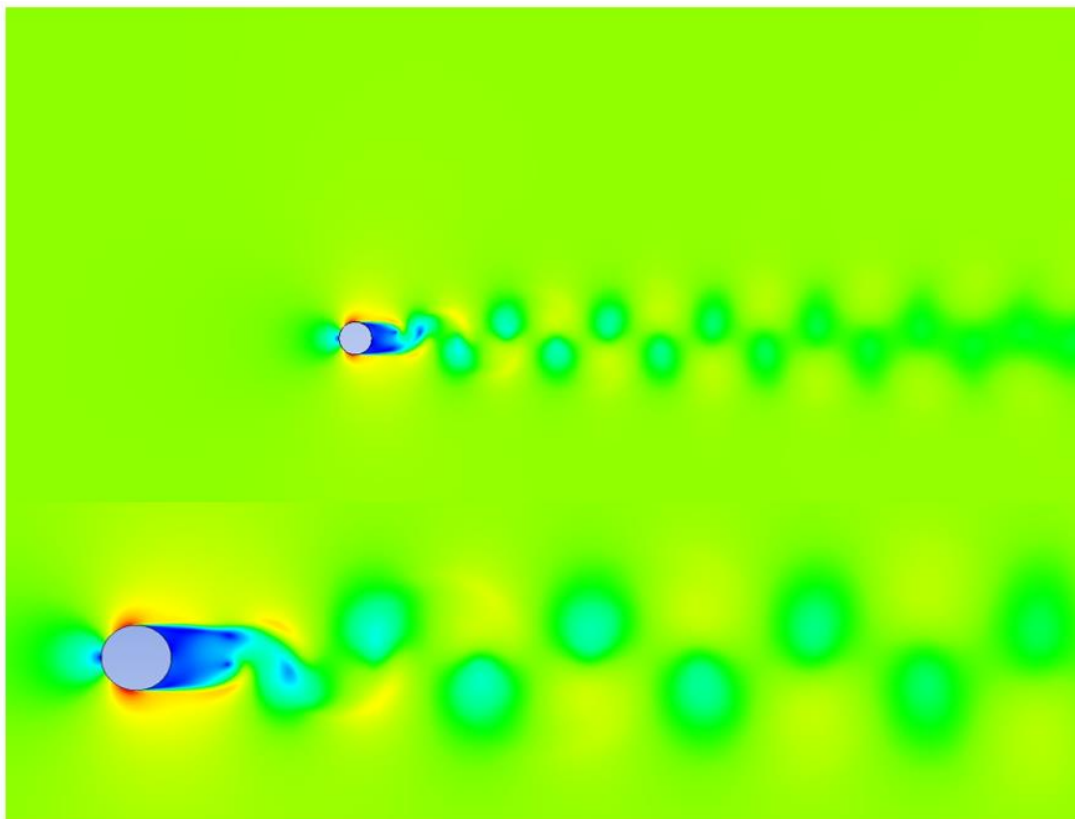
Figure 3.
Vortex-Shedding Contours.

3. Structural Modes

The structural modes of BWT can be tailored and determined either through analytical methods or by employing the FEM. In this context, the BWT is typically approximated as a beam model, and its natural modes are obtained using the FEM. This approach allows for the accurate prediction of the BWT's dynamic behavior by calculating its natural frequencies and corresponding mode shapes. By tailoring these structural modes, designers can optimize the turbine to achieve resonance with the vortex shedding frequency, thereby maximizing its oscillations and energy capture efficiency.

Both the natural frequencies and mode shapes can be obtained by solving the eigenvalue problem,

$$\left(K - \omega^2 M \ddot{W}\right)W = 0 \tag{5}$$

here K and M are simply the mass and stiffness matrices of a beam element [18] wheras W is the lateral displacement vector. For the luck in phenomena to take place both the aerodynamic natural frequency and structural fundamental frequency must be identical. Figure 4 illustrates the 1st three modes of BWT1 in reference [8]. Here, the fundamental natural frequency is 3.2193 which is nearly equal the vortex shedding frequency for the same case which is 3.5833 Hz.
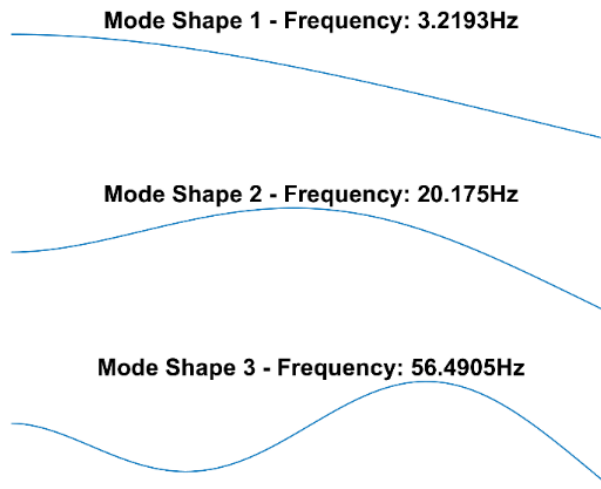

Figure 4.
BWT natural modes.

4. Model I – FE Aeroelastic Modeling

The aeroelastic analysis of BWT focuses on studying the interaction between aerodynamic forces, such as lift, and the elastic displacement of the turbine's structure. Unlike conventional structures such as aircraft wings and bridges, where resonance or flutter must be prevented to avoid structural failure [19-21] in BWTs, we aim to induce resonance. This intentional resonance amplifies the turbine's oscillations, thereby maximizing energy capture. To achieve this, it is essential to develop a detailed model that accurately predicts the interaction between aerodynamic forces and structural responses. Such a model can forecast resonance phenomena, allowing us to optimize the design and operational parameters of BWTs to enhance their vibrations and, consequently, maximize the power output. This aeroelastic analysis is crucial for ensuring that the BWT operates efficiently and effectively harnesses wind energy.

A simple approximation of bladeless wind turbines is to model them as a cantilever beam. The model is based on the coupling between the aerodynamic and structures, thus the structure and equation of motion can be defined as,

$$\frac{\partial^2}{\partial x^2}\left(EI\,\frac{\partial^2 W(x,t)}{\partial x^2}\right) + \rho_m A\,\frac{\partial^2 W(x,t)}{\partial t^2} = \frac{1}{2}\rho V_{air}^2 A_{surface}\,C_L(x,t) \tag{6}$$

ρ_m is the mast material density, A is the mast cross-section area, W is the blade displacement, $A_{surface}$ is the mast surface area ($A_{surface} = D_{m_{out}}L$ for a right cylindrical mast), $D_{m_{out}}$ is the mast outer diameter, L is the mast length, V_{air} is the air speed, and t represents the time.

The lift coefficient can be expressed in terms of an excitation component and blade velocity (stall term) based on Van der Pol equation, in the form [8].

$$C_L(x,t) = Q(x,t) - \frac{2\alpha}{D_{m_{out}}\,\omega_s}\,\dot{W}(x,t) \tag{7}$$

α is obtained based on empirical values. Q is the excitation component of the lift coefficient.

- ω_s is the vortex shedding frequency, $\omega_s = \frac{2\pi S V_{air}}{D}$, S is Strouhal number.

The aerodynamic excitation component Q can be obtained from the following 2nd order PDE,

$$\ddot{Q}(x,t) - \omega_s\, G\, (C_{L0}^2 - 4Q(x,t)^2)\dot{Q}(x,t) + \omega_s^2\, Q(x,t) = \omega_s F_p \frac{\dot{W}(x,t)}{D_{m_{out}}} \qquad (8)$$

F_p and G are empirical parameters. Equation 6 can be approximated using FEM in the form of [18],

$$M\ddot{W} + C\dot{W} + KW = F \qquad (9)$$

The BWT has been considered as a cantilever flexible hollow cylindrical beam with outer diameter $D_{m_{out}}$, thickness T and length L.

Equation 6 and Equation 9 represent the aerodynamic and structural equations of motion, respectively. Traditionally, these equations are solved using either a sinusoidal solution approach [7] or the Galerkin method [8]. In this work, *we present a novel solution methodology based on the FEM, implemented in two distinct models that incorporate different aerodynamic approaches and time integration techniques, as outlined below.*

Model I employs the finite difference method (FDM) to solve the time-dependent aerodynamic equations, and the Newmark method to solve the time-varying structural equations. For the aerodynamic PDE, time integration is performed using the FDM, based on a Taylor series approximation, as follows:

$$\ddot{Q}(x,t) = \omega_s\, G\, (C_{L0}^2 - 4Q(x,t)^2)\dot{Q}(x,t) - \omega_s^2\, Q(x,t) + \omega_s F_p \frac{\dot{W}(x,t)}{D_{m_{out}}} \qquad (10)$$

$$\dot{Q}(x,t) = \dot{Q}(x,t_{i-1}) + dt\, \ddot{Q}(x,t_{i-1}) \qquad (11)$$

$$Q(x,t) = Q(x,t_{i-1}) + dt\, \dot{Q}(x,t_{i-1}) + 0.5\, dt^2 \ddot{Q}(x,t_{i-1}) \qquad (12)$$

Here, the aerodynamic forces become

$$C_L = Q(x,t_i) + Q_h(x,t_i) - \frac{2\alpha}{\omega_s D_{m_{out}}}\dot{W}(x,t) \qquad (13)$$

C_L is the lift coefficient distribution over the blade, where Q_h is the homogenous solution.

The time dependence is integrated using Newmark method [22] a numerical technique widely employed in dynamic analyses. This method is particularly effective for solving linear systems under dynamic loading, as it enables the calculation of displacement, velocity, and acceleration over time. The time integration solution for the structural FE equation is derived as follows:

$$W_{eff} = W(x,t_{i-1}) + dt\, \dot{W}(x,t) + \left(\frac{1}{2} - \beta\right) dt^2\, \ddot{W}(x,t) \qquad (14)$$

$$F_{eff} = \frac{1}{2}\rho V_{air}^2 A_{surface}\, C_L \qquad (15)$$

$$K_{eff} = K + \frac{\gamma}{\beta\, dt} C + \frac{1}{\beta\, dt^2} M \qquad (16)$$

Where γ and β are the Newmark integration parameters [22].

$$W(x,t) = K_{eff}^{-1} F_{eff}$$

$$\dot{W}(x,t) = \frac{\gamma}{\beta\, dt}\Delta W(x,t) - \frac{\gamma}{\beta}\dot{W}(x,t) - \left(\frac{\gamma}{2\beta} - 1\right) dt * \ddot{W}(x,t) \qquad (17)$$

$$\ddot{W}(x,t) = \frac{1}{\beta\, dt^2}\Delta W(x,t) - \frac{1}{\beta\, dt}\dot{W}(x,t) - \frac{1}{2\beta}\ddot{W}(x,t)$$

The present aeroelastic model is applied to a typical BWT [8] with an outer diameter of 0.18 m, a thickness of 0.001 m, and a length of 4 m. The BWT is constructed from a material with a Young's Modulus of 2.2 GPa and a density of 1040 kg/m³. The air speed is 4.3 m/s to ensure the resonance phenomena to take place. The slender and lightweight design, coupled with the specified material properties, ensures that the turbine can oscillate effectively in response to vortex shedding induced by wind flow, thereby maximizing its energy capture potential. The chosen dimensions and material properties also influence the natural frequency of the system, which must be matched with the vortex shedding frequency for optimal performance. This study aims to explore the dynamic response and energy conversion efficiency of the BWT under these specified conditions.

The maximum displacement, lift coefficient, and aerodynamic force of the BWT are illustrated in the Figure 5, based on the present aeroelastic FE model. The displacement oscillates around 0.01 meters, indicating the turbine's consistent movement under aerodynamic excitation. The lift coefficient fluctuates between a value of 2, reflecting the varying aerodynamic lift forces acting on the structure. Additionally, the applied aerodynamic loads oscillate between 10 N, showcasing the dynamic loading conditions experienced by the turbine
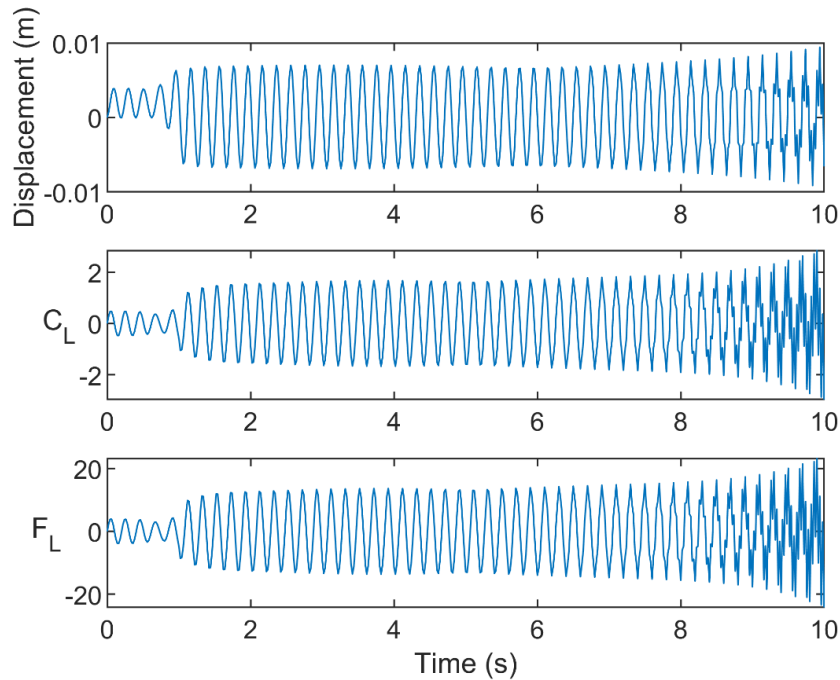
Figure 5.
Maximum displacement, lift coefficient, and force as a function of time.

The displacement distribution along the length of the BWT is depicted in Figure 6, indicating that the aeroelastic interaction takes place at the 1st mode. The maximum displacement observed is consistent with the values shown in Figure 5, highlighting the oscillation around 0.01 meters. At the blade root, the displacement is zero due to the fixed boundary conditions, which prevent movement at this point. Additionally, the figure illustrates the displacement time history, providing a detailed view of how the displacement evolves over time along the length of the BWT. This time history is essential for analyzing the dynamic response and ensuring that the turbine design can withstand the varying aerodynamic forces it encounters.
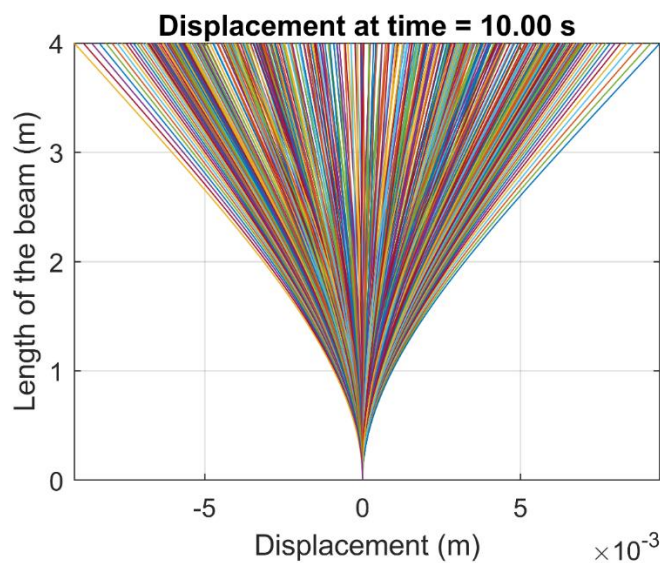

Figure 6.
The BWT displacement distribution.

5. Model II – Piezoelectric Integrated BWT

Piezoelectric energy harvesting is a process that converts mechanical energy, typically from vibrations, strain, or pressure, into electrical energy using piezoelectric materials. These materials generate an electric charge in response to applied mechanical stress, making them ideal for energy harvesting applications. Piezoelectric energy harvesters are used in various applications, including powering small electronic devices, sensors, wireless communication systems, and aeroelastic application, particularly in environments where traditional power sources are impractical [21, 23].

The principle behind piezoelectric energy harvesting involves materials like lead zirconate titanate (PZT), zinc oxide (ZnO), and polyvinylidene fluoride (PVDF). When these materials are subjected to mechanical deformation, they produce an electric field proportional to the applied force. This capability is exploited in different configurations, such as cantilever beams, where mechanical vibrations induce stress in the piezoelectric material, generating an electric output. This is a typical concept that can be applied to BWTs. Research and development in piezoelectric materials and device architectures continue to enhance the efficiency and practicality of piezoelectric energy harvesting. Innovations include improving material properties, optimizing device designs for specific applications, and integrating piezoelectric harvesters with energy storage systems to manage and utilize the generated power effectively.

Piezoelectric energy harvesting has been successfully implemented in several aeroelastic applications, including wings [11, 17, 24] flapping flag models [12] wind turbines [25] BWTs [9] and helicopter blades [26]. Typically, wings are designed to avoid flutter instability, but in the context of energy harvesting, achieving a stable flutter phenomenon is essential for maximizing power output. This stable flutter state is crucial as it allows for the extraction of maximum energy.

Various configurations have been explored in the literature for extracting energy from vibrating devices using piezoelectric materials. Among these, the flapping flag model stands out as one of the most efficient configurations for obtaining maximum power output [27]. The key parameter affecting the power output in this model is the tip mass in the flange. The properties of the tip mass, including its moment of inertia and center of gravity, are critical in determining the amount of energy that can be extracted [28, 29]. Adjusting these properties can significantly influence the efficiency and effectiveness of the energy harvesting system.

As part of the present work, we develop a novel FE model for piezoelectric energy harvesting using a plate-like BWT model. In this model, piezoelectric patches are strategically applied at the plate root, where the maximum strain occurs, to optimize energy conversion. A sinusoidal signal is applied to the plate, at tip, to simulate dynamic loading conditions, and the resulting charge generated by the piezoelectric patches is recorded. This innovative approach allows for a detailed analysis of the energy harvesting potential and provides insights into optimizing the placement and configuration of piezoelectric materials to maximize efficiency. The recorded data demonstrate the effectiveness of this method in capturing mechanical energy from aeroelastic vibrations and converting it into electrical energy, highlighting its potential for enhancing the performance of piezoelectric energy harvesting systems. A typical piezoelectric patch applied to cantilever plate in shown in Figure 7.

A harmonic displacement is applied to the plate tip to simulate the VIV aerodynamic loading conditions,

$$w = q_0 \sin(2\pi f t)$$
$$f = 1 \frac{cycle}{10} = 0.1 \, Hz \tag{18}$$
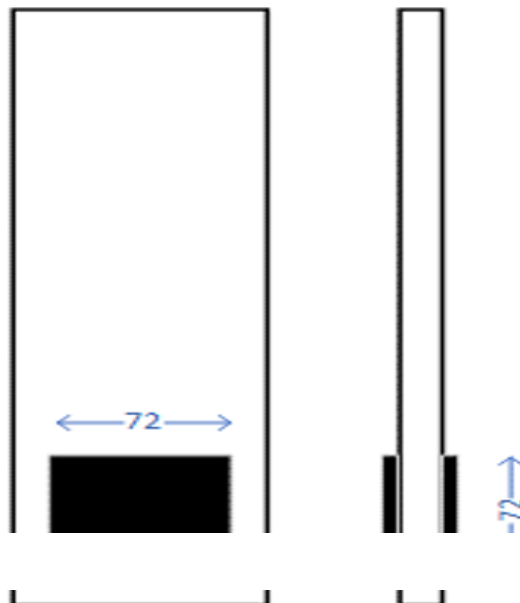
Figure 7.
Piezoelectric patches applied to the cantilever plate.
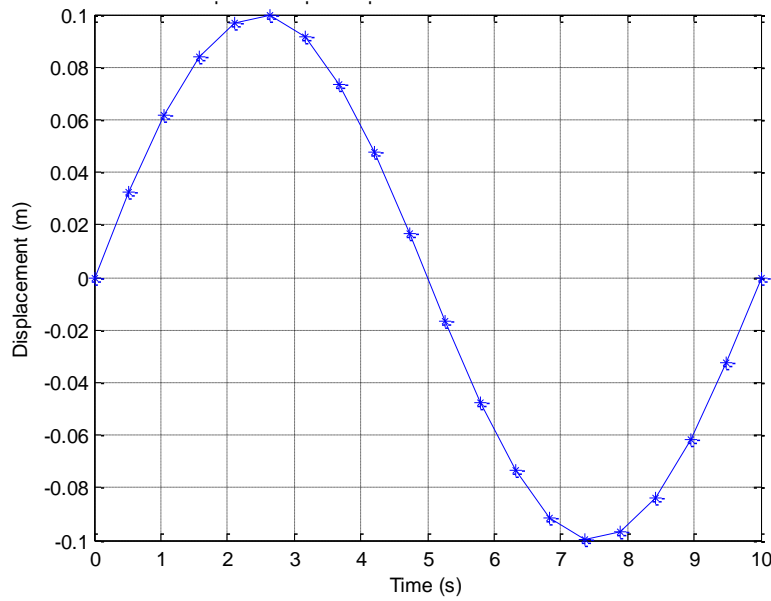
Figure 8.
Input harmonic displacement.

The FEM is based on the classical laminated plate theory [30]. Consider the linear equilibrium equation (equation of motion) [31]

$$\sigma_{ij,j} + f_i = \rho u_{,tt} \tag{19}$$

where f is the force per unit volume, σ is the Cauchy stress tensor, and u is the displacement. The stress-strain relation takes the form [32],

$$\sigma_{ij} = \lambda \, \delta_{ij} \, u_{k,k} + 2\mu \, u_{(i,j)}$$

where

$$w_{(i,j)} = \frac{w_{i,j} + w_{j,i}}{2} \tag{20}$$

λ and μ are Lame′ constants.

Equation *(20)* can be written in matrix form,

$$\sigma = D \, \varepsilon \tag{21}$$

Where D is the material stiffness. A 4-note quadrilateral element is utilized in the present analyses (see Figure 9) [20, 21].
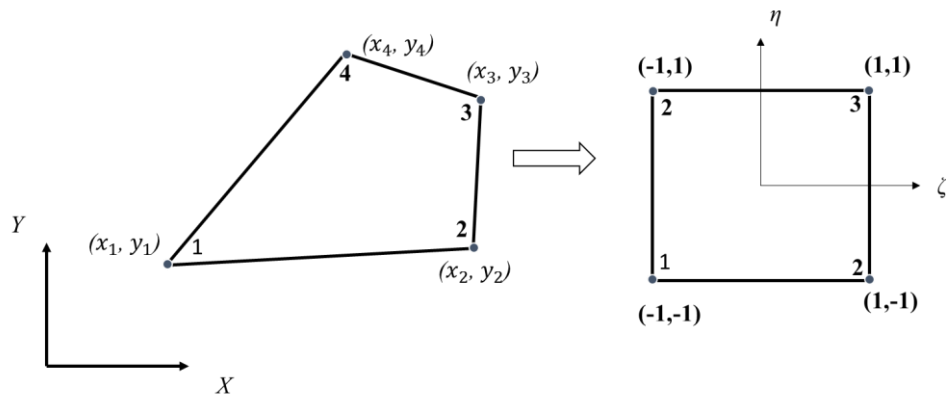

Figure 7.
4-node shell element

Then, the finite element equation can be written as

$$M^e \ddot{q} + C^e \, \dot{q} + K^e q = F^e \tag{22}$$

M^e denotes the element mass matrix, C^e represents the element damping matrix, K^e is the element stiffness matrix, q signifies the nodal displacements, and F^e is the nodal force vector.

1.

The piezoelectric charge is determined based on the following equation,

$$Q(t) = 2 \sum_{j=1}^{Ne} \frac{1}{2} \left[\iint_{-1}^{1} e(2B_p - (Z_k + Z_{k+1})B_b) |J| d\xi d\eta \right] \{q_j^e\} \tag{23}$$

e is the piezoelectric stiffness matrix, B_p the strain-displacement matrix for inplane action, and B_b is the strain displacement matrix for bending action.

Figure 8.
Piezoelectric configuration over the plate.

The piezoelectric current is obtained from,

$$i(t) = \frac{dq(t)}{dt} \approx \frac{q(t+1) - q(t)}{\Delta t} \tag{24}$$

A state-space model is developed for the FE equations incorporating the piezoelectric effect. The state-space representation of the system includes state variables, and output equations for the PZT sensor. This representation is beneficial for solving time-dependent problems as it allows for more efficient and stable numerical integration. By structuring the system in state-space form, the dynamic behavior of the piezoelectric elements can be accurately captured, facilitating the analysis of the energy harvesting performance. The state-space model enables a systematic approach to handle the complexities of coupled electromechanical systems, ensuring precise prediction of the system's response under dynamic loading.

The state space model can be represented as following,

$$\dot{X} = AX + Bu \tag{25}$$

$$Y = CX \tag{26}$$

where

A	State matrix
B	State control matrix
X	State vector
u	Control vector
Y	Output vector

The state-space matrices are defined as,

$$A = \begin{bmatrix} [0] & [I] \\ -M^{-1}K & -M^{-1}C \end{bmatrix}, B = \begin{bmatrix} 0 \\ -M \end{bmatrix}, X = \begin{Bmatrix} q \\ \dot{q} \end{Bmatrix} \tag{27}$$

The state-space model is then solved using MATLAB and applied to a plate-like BWT with a length of 4 m and a width of 0.15 meters. The plate is constructed from steel, with a Young's Modulus of 200 GPa, a Poisson's ratio of 0.3, and a density of 7580 kg/m³. It has a thickness of 0.6 mm. For the present analyses, a typical piezoelectric sheet from piezo-

systems [33] is utilized. This setup allows for an accurate simulation of the piezoelectric energy harvesting capabilities of the BWT, leveraging the robust computational power of the model to handle the complex dynamics of the system. Three cases have been considered for the present analyses:

Case 01 – Sandwich PZT plate model with tip sinusoidal excitation

Case 02 – Sandwich PZT plate model with mid-span sinusoidal excitation (0.8675 m from root).

Case 03 – Sandwich PZT plate model with mid-span sinusoidal excitation and tip point mass (5 kg).
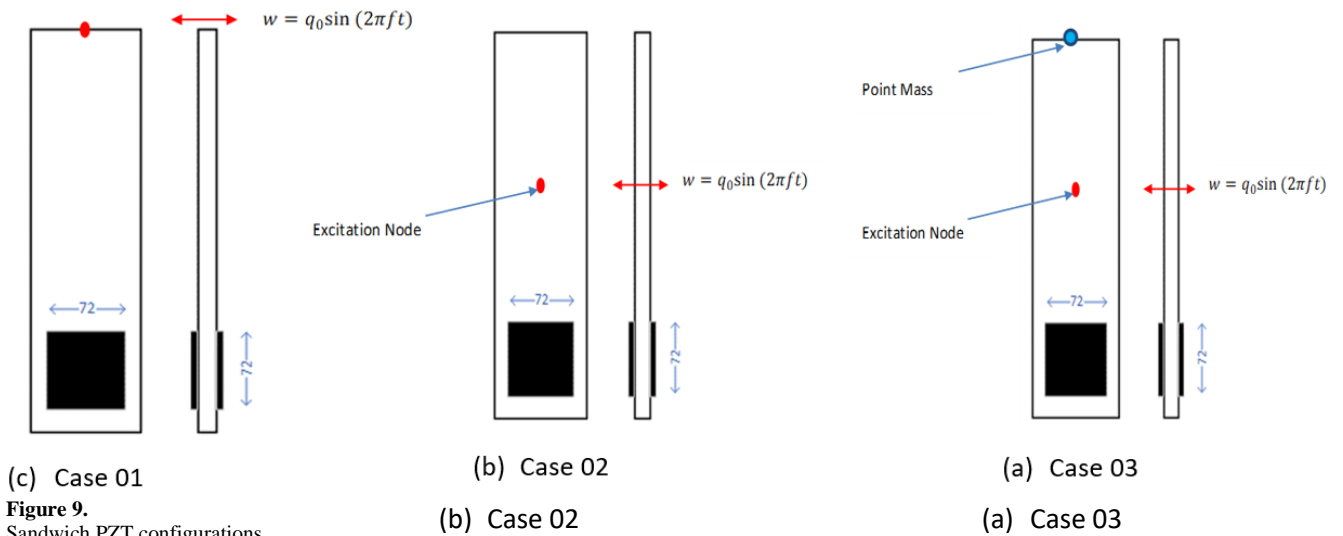
Figure 9.
Sandwich PZT configurations.

The piezoelectric sensor material properties are listed in Table 1.

Table 1.
PZT material properties.

Property	PZT – G1195N
Young's Moduli E_{11} [Gpa]	63
E_{22}	63
Poisson's ratio v_{12}	0.3
Shear moduli G_{12} [Gpa]	24.2
Density ρ [kh/m^3]	7600
Piezoelectric constants [C/m^2] $e_{31} = e_{32}$	22.86
$\boldsymbol{d_{31}}$	-190E-12

Three smart plate cases are conducted, each with single and double PZT patches subjected to four different excitation frequencies, resulting in a total of 12 models as illustrated in Figure 14 and Figure 15. The excitation frequency significantly influences both the peaks and the distribution of the output charge over time. Notably, the maximum charge amplitude occurs at excitation frequencies of 4.86 Hz which is equal the 2nd natural frequency of the plate. This analysis demonstrates how varying the excitation frequency can affect the performance of piezoelectric energy harvesting systems, providing insights into optimizing the configuration and operational conditions to maximize energy output.

The natural frequencies and mode shapes for Case 01 and Case 02 are illustrated in Figure 12, while those for Case 03, which includes a point mass, are shown in Figure 13. The addition of a tip mass decreases the natural frequencies of the plate, which is an expected outcome due to the increased inertia. Natural frequencies are crucial in the design and operation of BWTs because the system is typically excited at these frequencies to maximize vibrational displacement and, consequently, the output power. The design of the BWT aims to have a natural frequency that closely matches the aerodynamic vortex shedding frequency. This alignment ensures that the BWT can effectively harness the energy from the induced vibrations. For this reason, we will excite the current plate-like BWT at both the lower frequency and the second mode natural frequency.
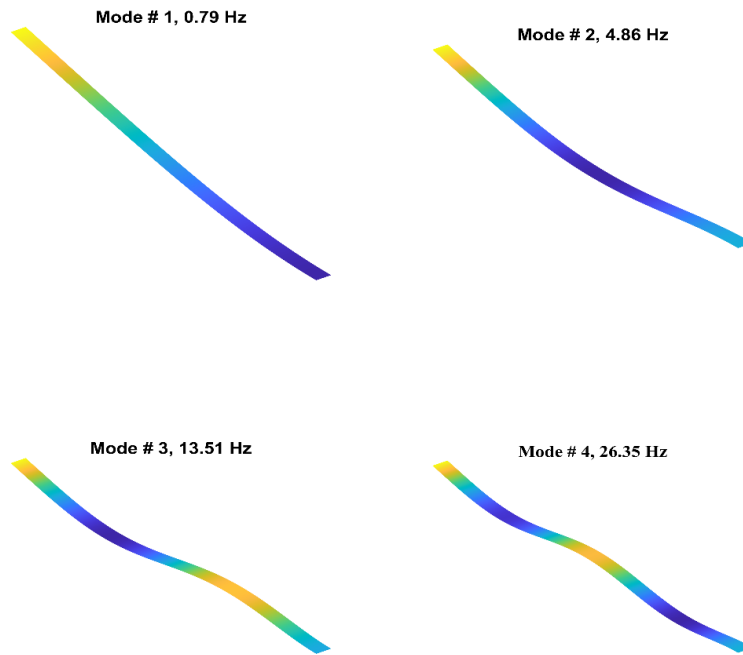
Figure 10.
Natural frequencies and mode shapes Case 01.
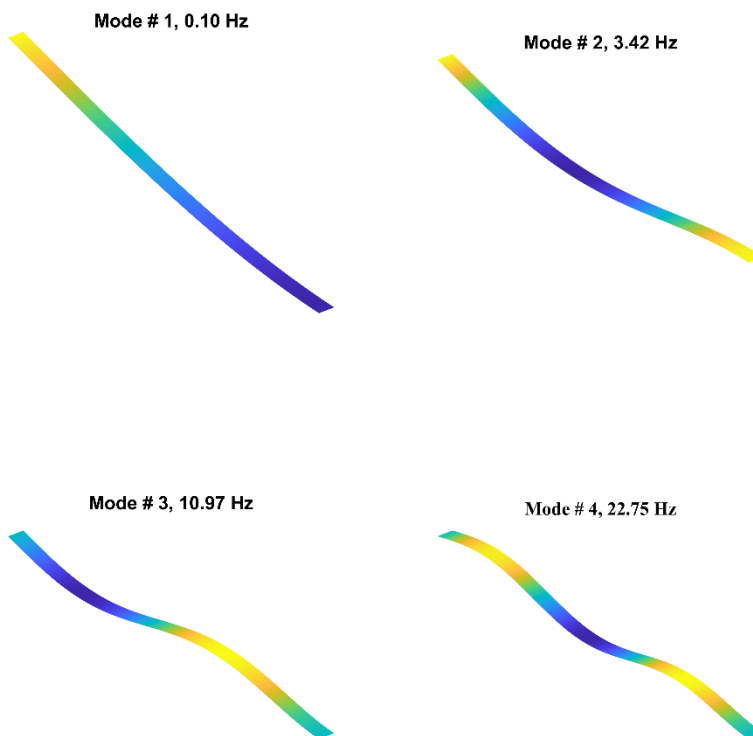
Figure 11.
Natural frequencies and mode shapes for Case 03.
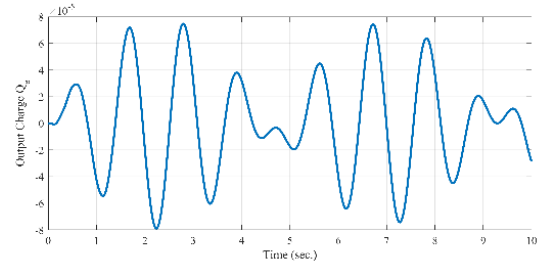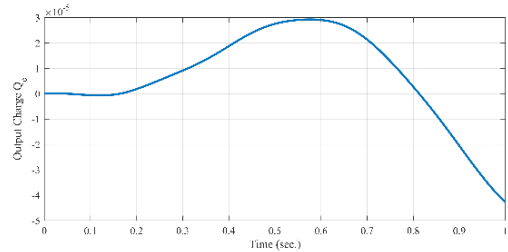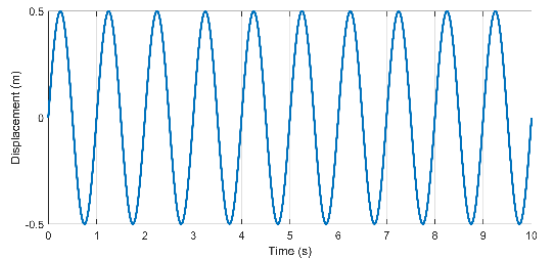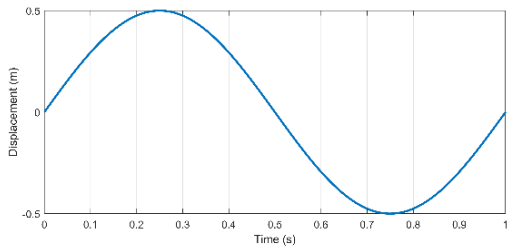
a. 1Hz – 1sec

b. 1Hz – 10sec
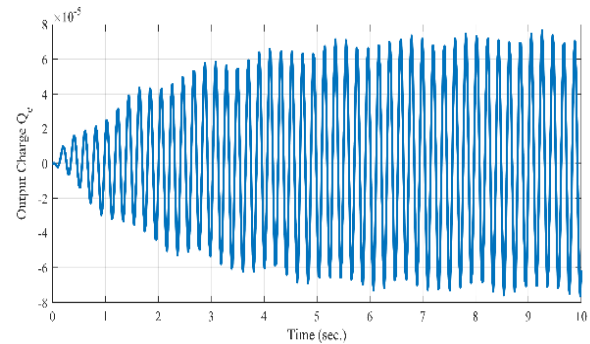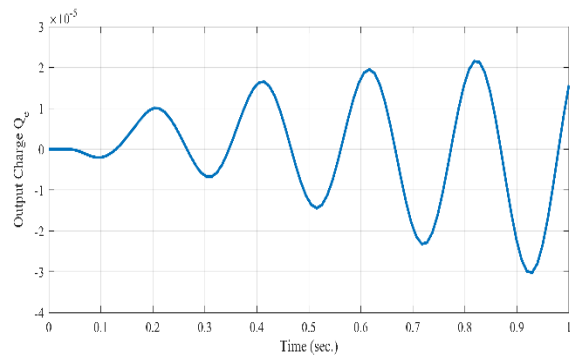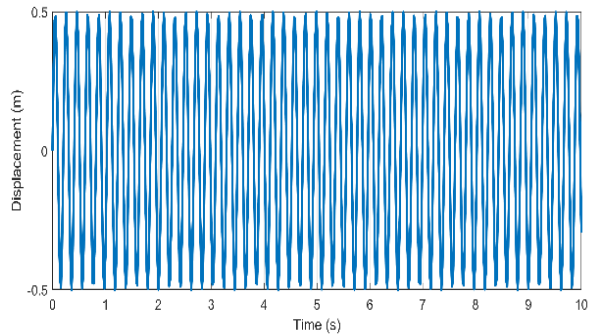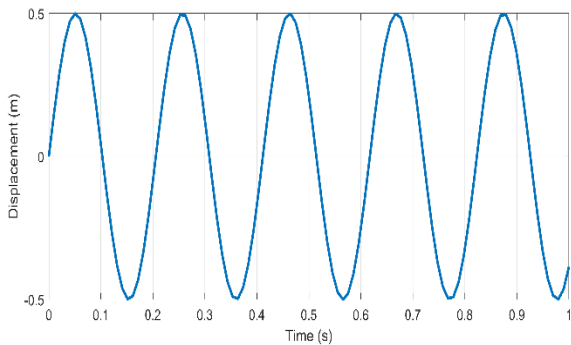
c. 4.86Hz – 1sec

d. 4.86Hz – 10sec

Figure 12.
Case 01 sandwich PZT-plate model under sinusoidal load with different excitation frequencies and time.

Figure 15 illustrates the effect of the tip mass on the output charge of the smart plate. It is observed that the presence of a tip mass decreases the output charge for excitation frequencies of 1 Hz however it increases the output charge at resonance frequency (3.42 Hz), enhancing the energy harvesting efficiency at this frequency. This indicates a frequency-dependent behavior where the tip mass can either augment or diminish the harvested energy. The findings underscore the importance of optimizing the tip mass for specific operational frequencies to maximize the performance of piezoelectric energy harvesting systems. This behavior can be attributed to the changes in dynamic response and resonance characteristics introduced by the added mass at the plate tip.
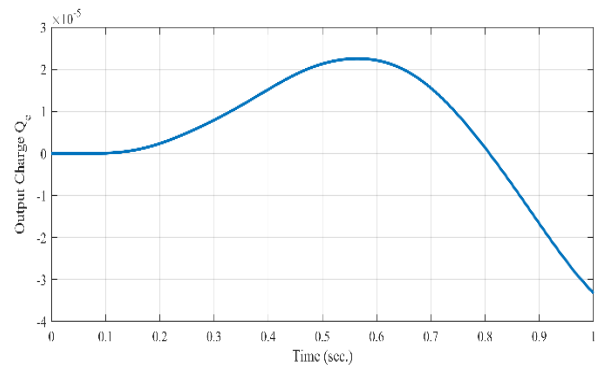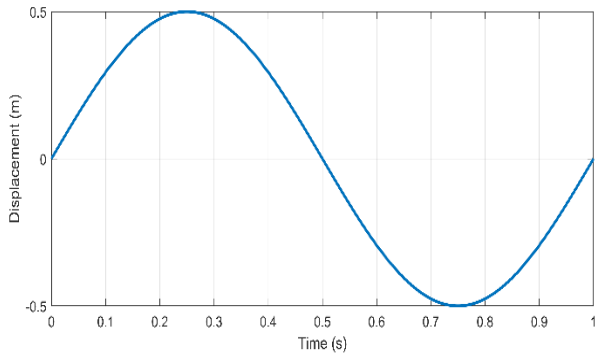
Case 02　　　　　　　　　　　　　　　　　　　　Case 03
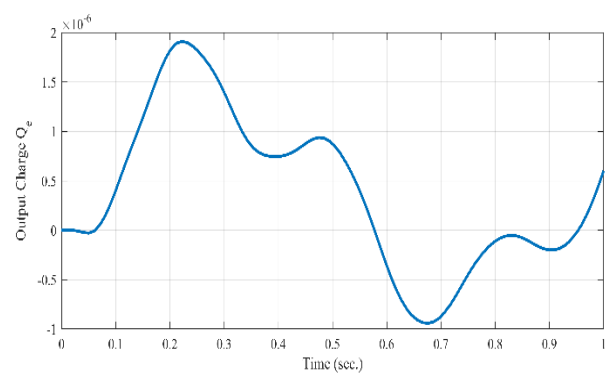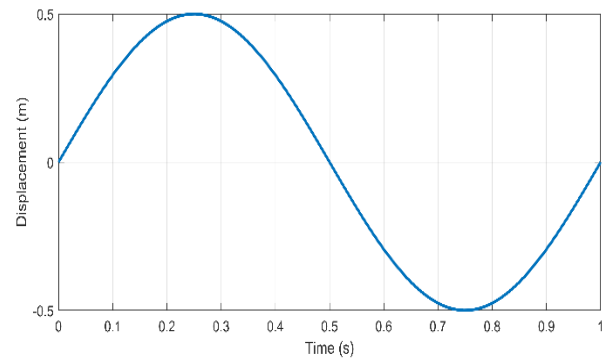
Excitation frequency 1 Hz – 1 sec
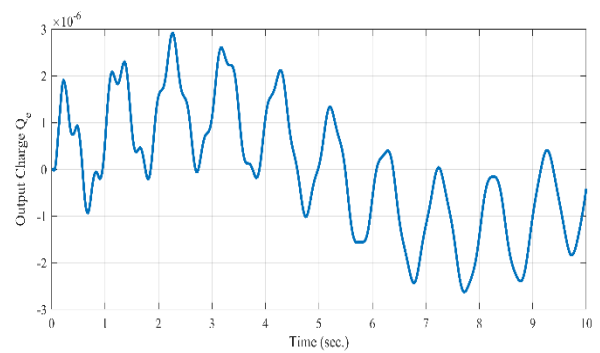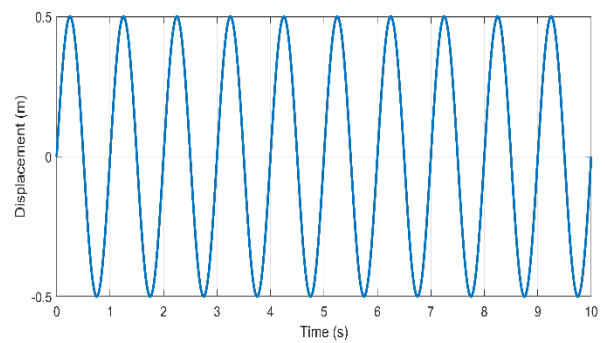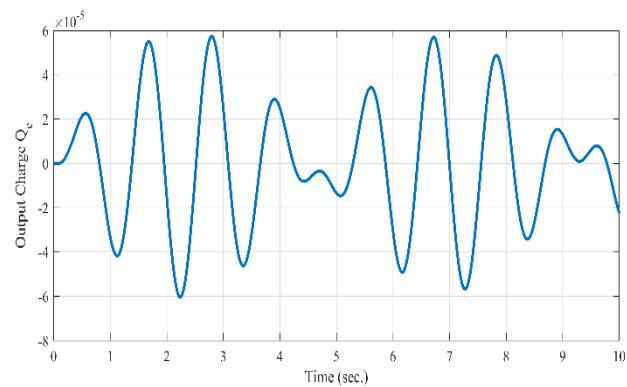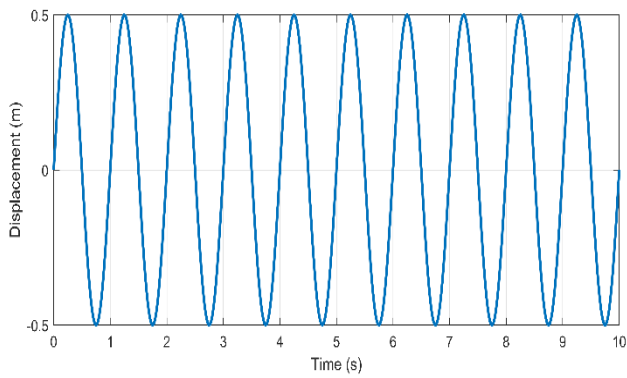
Excitation frequency 1 Hz – 10 sec
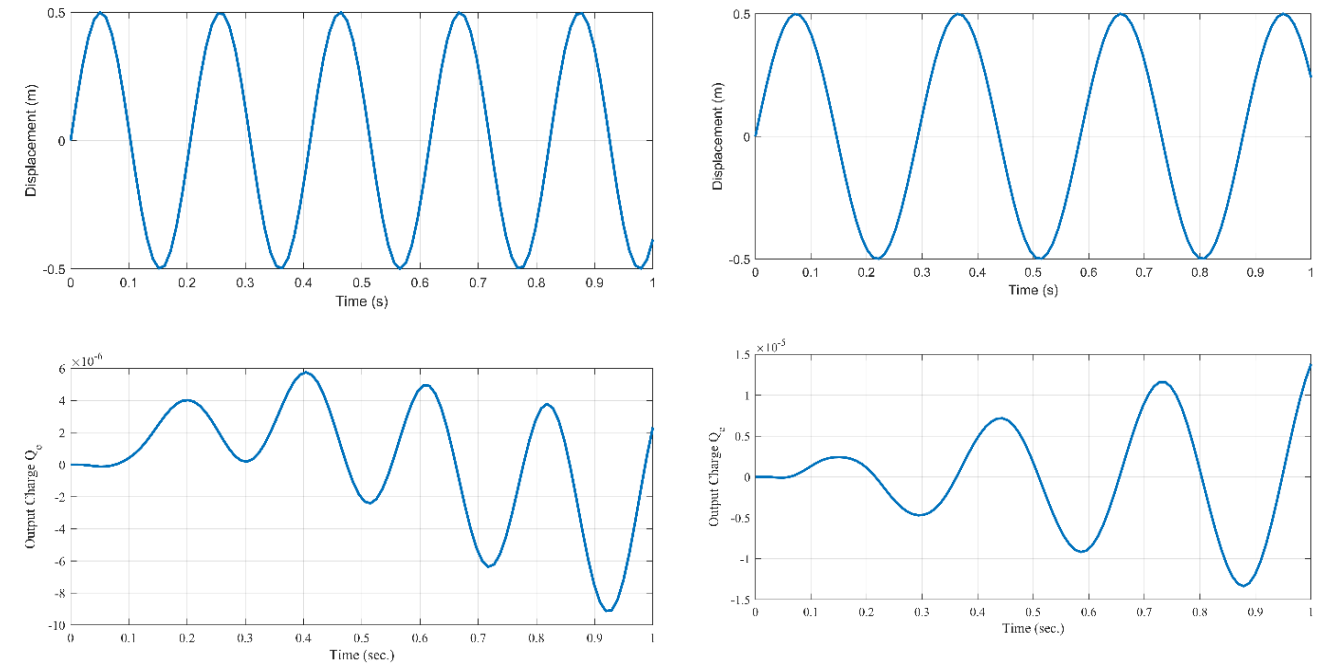
Excitation frequency 4.86(left) Hz and 3.42Hz (right) – 1 sec
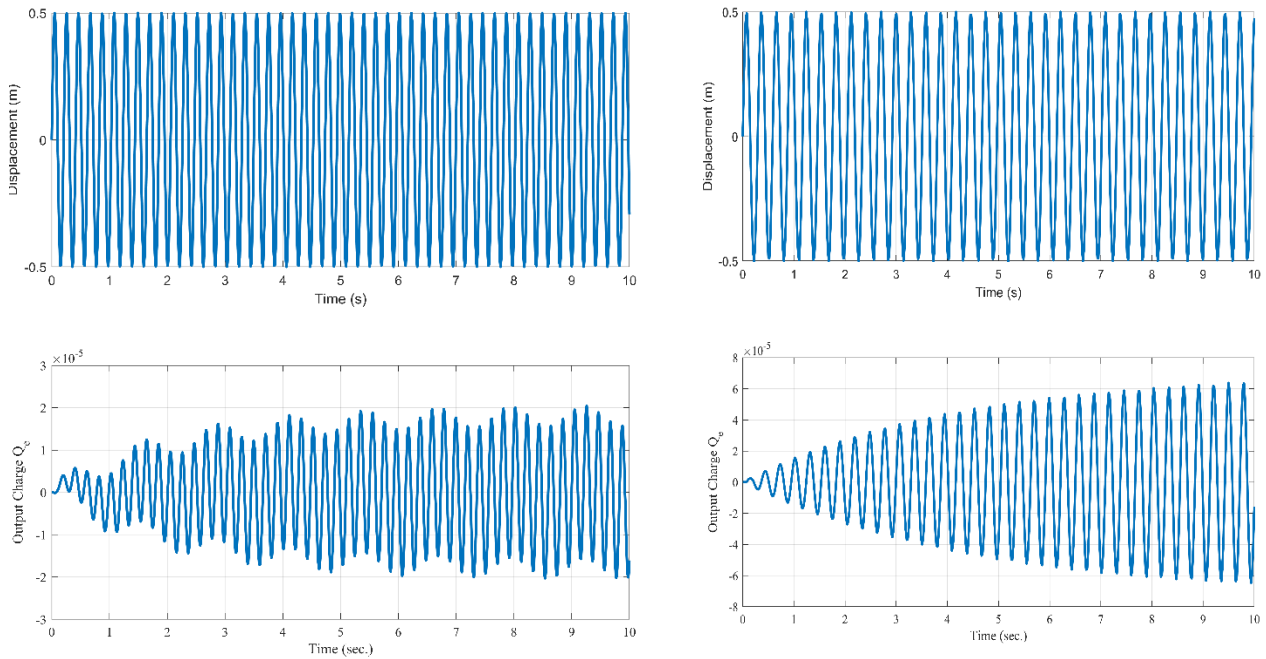
Excitation frequency 4.86(left) Hz and 3.42Hz (right) – 10 sec

Figure 13.
Plate displacement and output charge with and without tip mass.

6. Conclusion and Future Work

In this study, two FE models are developed and applied to simplified BWTs models to address distinct yet interconnected aspects: aeroelastic analysis and piezoelectric energy harvesting. The aeroelastic model successfully captured the interaction between aerodynamic loads and the BWT structure, utilizing a semi-empirical wake oscillator model to simulate realistic aerodynamic forces. This model proved effective in predicting the aeroelastic characteristics of BWTs, offering valuable insights into their stability and dynamic behavior under various wind conditions.

The second model focused on the piezoelectric energy harvesting potential of BWTs. By applying sinusoidal aerodynamic loads that simulate the aerodynamic loads, this model predicted the charge generated by piezoelectric patches placed at the root of a plate-like BWT. The results demonstrated the efficiency of the model in simulating the energy conversion process, highlighting the feasibility of harnessing electrical energy from the mechanical vibrations of BWTs.

Both models make significant contributions to the advancement of renewable energy, particularly in optimizing bladeless wind turbine (BWT) designs. The aeroelastic model plays a crucial role in ensuring structural stability and enhancing performance, while the piezoelectric energy harvesting model introduces new possibilities for efficient energy generation. Together, these models create a comprehensive framework for improving BWT efficiency and expanding their

applicability in sustainable energy systems. Future research could focus on further refining these models and exploring their integration into real-world applications. The beam finite element (FE) model has proven to be effective in predicting the BWT's lift and vibration displacement along its length. Additionally, results indicate that the presence of a tip mass decreases the output charge at an excitation frequency of 1 Hz but significantly enhances energy harvesting efficiency at the resonance frequency (3.42 Hz), demonstrating its potential to improve power generation at optimal operational conditions.

For future work, the two models should be combined to develop a more advanced and robust aero-piezoelectric model for the stability, dynamics, and piezoelectric analysis of BWTs. This integrated model needs to incorporate a more sophisticated aerodynamic framework that relies on precise aerodynamic calculations rather than empirical values. By addressing the limitations of current empirical approaches, the combined model will enhance the accuracy of simulations and predictions related to the aerodynamic loads, structural responses, and energy harvesting capabilities of BWTs. This advanced aero-piezoelectric model will be instrumental in optimizing the design and performance of BWTs, leading to more efficient and reliable renewable energy solutions.

References

[1]   I. Bahadur, "Dynamic modeling and investigation of a tunable vortex bladeless wind turbine," *Energies,* vol. 15, no. 18, p. 6773, 2022. https://doi.org/10.3390/en15186773

[2]   E. González-González, D. J. Yáñez, S. Del Pozo, and S. Lagüela, "Optimizing bladeless wind turbines: Morphological analysis and lock-in range variations," *Applied Sciences,* vol. 14, no. 7, p. 2815, 2024. https://doi.org/10.3390/app14072815

[3]   R. Tandel, S. Shah, and S. Tripathi, "A state-of-art review on bladeless wind turbine," *Journal of Physics: Conference Series,* vol. 1950, no. 1, p. 012058, 2021. https://doi.org/10.1088/1742-6596/1950/1/012058

[4]   G. Parkinson, "Phenomena and modelling of flow-induced vibrations of bluff bodies," *Progress in Aerospace Sciences,* vol. 26, no. 2, pp. 169-224, 1989. https://doi.org/10.1016/0376-0421(89)90008-0

[5]   E. Berger, "On a mechanism of vortex-excited oscillations of a cylinder," *Journal of Wind Engineering and Industrial Aerodynamics,* vol. 30, no. 3, pp. 301–310, 1988.

[6]   R. Skop and O. Griffin, "A model for the vortex-excited resonant response of bluff cylinders," *Journal of Sound and Vibration,* vol. 27, no. 2, pp. 225-233, 1973. https://doi.org/10.1016/0022-460X(73)90063-1

[7]   R. A. Skop and S. Balasubramanian, "A new twist on an old model for vortex-excited vibrations," *Journal of Fluids and Structures,* vol. 11, no. 4, pp. 395-412, 1997. https://doi.org/10.1006/jfls.1997.0085

[8]   A. Chizfahm, E. A. Yazdi, and M. Eghtesad, "Dynamic modeling of vortex induced vibration wind turbines," *Renewable Energy,* vol. 121, pp. 632-643, 2018. https://doi.org/10.1016/j.renene.2018.01.038

[9]   A. Younis, Z. Dong, M. ElBadawy, A. AlAnazi, H. Salem, and A. AlAwadhi, "Design and development of bladeless vibration-based piezoelectric energy–harvesting wind turbine," *Applied Sciences,* vol. 12, no. 15, p. 7769, 2022. https://doi.org/10.3390/app12157769

[10]   A. Abdelkefi, A. Nayfeh, and M. Hajj, "Design of piezoaeroelastic energy harvesters," *Nonlinear Dynamics,* vol. 68, pp. 519-530, 2012. https://doi.org/10.1007/s11071-011-0233-x

[11]   A. Abdelkefi, M. R. Hajj, and A. H. Nayfeh, "Sensitivity analysis of piezoaeroelastic energy harvesters," *Journal of Intelligent Material Systems and Structures,* vol. 23, no. 13, pp. 1523-1531, 2012. https://doi.org/10.1177/1045389X12440752.

[12]   J. Dunnmon, S. Stanton, B. Mann, and E. Dowell, "Power extraction from aeroelastic limit cycle oscillations," *Journal of Fluids and Structures,* vol. 27, no. 8, pp. 1182-1198, 2011. https://doi.org/10.1016/j.jfluidstructs.2011.02.003.

[13]   H. D. Akaydin, N. Elvin, and Y. Andreopoulos, "Energy harvesting from highly unsteady fluid flows using piezoelectric materials," *Journal of Intelligent Material Systems and Structures,* vol. 21, no. 13, pp. 1263-1278, 2010. https://doi.org/10.1177/1045389X10366317

[14]   C. Bruni, J. Gibert, G. Frulla, E. Cestino, and P. Marzocca, "Energy harvesting from aeroelastic vibrations induced by discrete gust loads," *Journal of Intelligent Material Systems and Structures,* vol. 28, no. 1, pp. 47-62, 2017. https://doi.org/10.1177/1045389X16642533

[15]   A. Abdelkefi, A. Nayfeh, and M. Hajj, "Enhancement of power harvesting from piezoaeroelastic systems," *Nonlinear Dynamics,* vol. 68, pp. 531-541, 2012. https://doi.org/10.1007/s11071-011-0234-9

[16]   U. Javed, A. Abdelkefi, and I. Akhtar, "An improved stability characterization for aeroelastic energy harvesting applications," *Communications in Nonlinear Science and Numerical Simulation,* vol. 36, pp. 252-265, 2016. https://doi.org/10.1016/j.cnsns.2015.12.001

[17]   O. Doaré and S. Michelin, "Piezoelectric coupling in energy-harvesting fluttering flexible plates: Linear stability analysis and conversion efficiency," *Journal of Fluids and Structures,* vol. 27, no. 8, pp. 1357-1375, 2011. https://doi.org/10.1016/j.jfluidstructs.2011.04.008

[18]   D. L. Logan, *A first course in the finite element method*. United States: Thomson, 2007.

[19]   M. Mahran, H. Negm, and A. El-Sabbagh, "Aero-elastic characteristics of tapered plate wings," *Finite Elements in Analysis and Design,* vol. 94, pp. 24-32, 2015. https://doi.org/10.1016/j.finel.2014.09.009

[20]   M. Mahran, A. ELsabbagh, and H. Negm, "A comparison between different finite elements for elastic and aero-elastic analyses," *Journal of Advanced Research,* vol. 8, no. 6, pp. 635-648, 2017. https://doi.org/10.1016/j.jare.2017.06.009

[21]   M. M. Kasem and E. H. Dowell, "A study of the natural modes of vibration and aeroelastic stability of a plate with a piezoelectric material," *Smart Materials and Structures,* vol. 27, no. 7, p. 075043, 2018. https://doi.org/10.1088/1361-665X/aac8a7

[22]   F. Bamer *et al.*, "A newmark space-time formulation in structural dynamics," *Computational Mechanics,* vol. 67, no. 5, pp. 1331-1348, 2021. https://doi.org/10.1007/s00466-021-01989-4

[23]   M. M. Kasem, H. Negm, and A. Elsabbagh, "Aeroelastic modeling of smart composite wings using geometric stiffness," *Journal of Aerospace Engineering,* vol. 32, no. 2, p. 04018143, 2019. https://doi.org/10.1061/(ASCE)AS.1943-5525.0000957

[24] A. Erturk, O. Bilgen, M. Fontenille, and D. J. Inman, "Piezoelectric energy harvesting from macro-fiber composites with an application to morphing-wing aircrafts," in *Proceedings of the 19th International Conference on Adaptive Structures and Technologies, Ascona, Switzerland*, 2008, pp. 6–9.

[25] V. Thirusangu and K. M. Parammasivam, "A CFD analysis of controlled flutter phenomenon," *Thermal Science,* vol. 20, pp. S955–S965, 2016. https://doi.org/10.2298/TSCI16S4955T

[26] M. Bryant, A. Fang, and E. Garcia, "Self-powered smart blade: Helicopter blade energy harvesting," presented at the The Active and Passive Smart Structures and Integrated Systems , International Society for Optics and Photonics, 2010.

[27] M. Bryant and E. Garcia, "Modeling and testing of a novel aeroelastic flutter energy harvester," *Journal of Vibration and Acoustics,* vol. 133, no. 1, p. 011010, 2011. https://doi.org/10.1115/1.4002788

[28] M. Bryant, E. Wolff, and E. Garcia, "Aeroelastic flutter energy harvester design: The sensitivity of the driving instability tosystem parameters," *Smart Materials and Structures,* vol. 20, no. 12, p. 125017, 2011. https://doi.org/10.1088/0964-1726/20/12/125017

[29] M. Bryant, E. Wolff, and E. Garcia, "Parametric design study of an aeroelastic flutter energy harvester," presented at the The Active and Passive Smart Structures and Integrated Systems 2011, International Society for Optics and Photonics, 2011.

[30] K. Lam, X. Peng, G. Liu, and J. Reddy, "A finite-element model for piezoelectric composite laminates," *Smart Materials and Structures,* vol. 6, no. 5, p. 583, 1997.

[31] T. J. Hughes, *The finite element method*. United States: Prentice-Hall, 1987.

[32] P. L. Gould, *Introduction to linear elasticity*. New York: Springer. https://doi.org/10.1007/978-1-4614-4833-4, 2013.

[33] Piezo Systems, "Piezo systems," Retrieved: http://www.piezo.com/, 2018.